Hindawi
Complexity
Volume 2019, Article ID 5803506, 13 pages
https://doi.org/10.1155/2019/5803506

WILEY | Hindawi

*Research Article*

# A New 4D Chaotic System with Two-Wing, Four-Wing, and Coexisting Attractors and Its Circuit Simulation

**Lilian Huang, Zefeng Zhang, Jianhong Xiang, and Shiming Wang**

*College of Information and Communication Engineering, Harbin Engineering University, Harbin 150001, China*

Correspondence should be addressed to Lilian Huang; lilian_huang@163.com

Received 16 July 2019; Revised 9 September 2019; Accepted 19 September 2019; Published 29 October 2019

Guest Editor: Serdar Çiçek



In order to further improve the complexity of chaotic system, a new four-dimensional chaotic system is constructed based on Sprott B chaotic system. By analyzing the system's phase diagrams, symmetry, equilibrium points, and Lyapunov exponents, it is found that the system can generate not only both two-wing and four-wing attractors but also the attractors with symmetrical coexistence, and the dynamic characteristics of the new system constructed are more abundant. In addition, the system is simulated by Multisim software, and the simulation results show that the results of circuit simulation and numerical simulation analysis are basically the same.

## 1. Introduction

Chaos is a complex, apparently random, and often surprising behavior in simple nonlinear dynamical systems [1]. Chaos, as a unique form of motion in nonlinear dynamic systems, is widely used in electronic engineering [2], information engineering [3], and other fields [4–6] because of its initial value sensitivity, boundedness, and inherent randomness [7]. In 1963, American meteorologist Lorenz put forward the first chaotic system model [8], which attracted wide attention of the scientific community, and then, new chaotic systems were constantly discovered. In 1976, Rössler proposed a new system named Rössler chaotic system [9], which had a different topology from Lorenz system. Chua proposed Chua's circuit in 1986 [10, 11], which was one of the simplest chaotic oscillation circuits. In 1994, Sprott constructed several different simple chaotic systems [12]. In 1999, Chen and Ueta . discovered the Chen system while studying the anticontrol of chaos [13]. In 2002, Lü et al. proposed a kind of transition system named Lü system which connected Lorenz and Chen systems [14]. In 2003, Liu and Chen constructed the first four-wing butterfly chaotic attractor [15], which attracted many researchers' attention. To improve the security of chaotic secure communication and chaotic information encryption, more and more researchers began to find chaotic systems with more complex dynamic behaviors [16–21].

In recent years, coexisting attractors had gradually become a research hotspot [22–24]. Compared with general chaotic attractors, the dynamic behaviors of coexisting attractors are more complex. In order to improve the security of information and reduce the possibility of information being decoded, coexisting attractors are more and more used in the field of encryption [25, 26]. In 2013, Li and Sprott proposed a multistable system with coexisting attractors [27] and found that the dynamic of the equilibrium points of the system depended on its stability and system structure. In 2014, Li and Sprott discovered a coexisting hidden attractor on a simple 4D Lorenz system [28], which had a large parameter region on a quasiperiodic torus. In 2017, Lai et al. proposed a unique 4D autonomous system with a signum function term [29], which can generate various types of coexisting attractors. In 2019, Zhou et al. proposed a chaotic system with multiple asymmetric coexisting attractors [30] and carried out circuit simulation and pulse synchronization research.

In this paper, a new 4D chaotic system based on Sprott B system is proposed. It includes the following elements: (i) It contains eight terms, including three nonlinear terms and one constant term. (ii) It is symmetric about the $z$-axis.

(iii) It can produce two-wing and four-wing attractors at the same time. (iv) It can also produce symmetric coexisting attractors. (v) The realization of the system circuit in physics is verified by the circuit simulation software, which is favorable for future engineering applications. This paper is organized as follows: In Section 2, a new chaotic system is proposed, and the coexistence of two-wing and four-wing attractors is observed through phase diagrams. In Section 3, we analyze its dynamic behaviors by symmetry, equilibrium points, bifurcation diagrams, Lyapunov exponents, and trajectory diagrams and introduce its symmetric coexisting attractors. An electronic circuit is designed in Section 4, and the correctness of the theoretical analysis is verified by circuit simulation experiment. Finally, the conclusion of this paper is given in Section 5.

## 2. A New Four-Dimensional Chaotic System

In this section, we mainly design the new chaotic system, and the new system proposed in this paper is described as follows:

$$\begin{cases} \dot{x} = a(y - x), \\ \dot{y} = xz + w, \\ \dot{z} = b - xy, \\ \dot{w} = yz - cw, \end{cases} \tag{1}$$

where positive real numbers $a$, $b$, and $c$ are system parameters and $x$, $y$, $z$, and $w$ are state variables. The new system (1) adds a state-feedback controller on the Sprott B chaotic system. Set $a = 6$, $b = 11$, and $c = 5$; the chaotic system can be generated. By calculation, the Lyapunov exponents are $\mathrm{LE}_1 = 0.5162$, $\mathrm{LE}_2 = -0.0001$, $\mathrm{LE}_3 = -4.9208$, and $\mathrm{LE}_4 = -6.5954$. The corresponding Lyapunov exponential dimension is as follows:

$$\begin{aligned} D_{\mathrm{L}} &= j + \frac{1}{\left|\mathrm{LE}_{j+1}\right|} \sum_{i=1}^{j} \mathrm{LE}_i \\ &= 3 + \frac{\mathrm{LE}_1 + \mathrm{LE}_2 + \mathrm{LE}_3}{\left|\mathrm{LE}_4\right|} \\ &= 3 + \frac{0.5162 - 0.0001 - 4.9208}{|-6.5954|} \\ &= 2.3322. \end{aligned} \tag{2}$$

Therefore, the attractor of the new system is a strange attractor with fractal dimension. Select the initial value $(x, y, z, w) = (10, 10, 0, 0)$. Through numerical simulation, we can get the chaotic attractors of system (1) as shown in Figure 1. As can be seen from Figure 1, system (1) presents two-wing butterfly chaotic attractors in the $x - y$, $x - z$, $y - z$, and $z - w$ phase planes. The four-wing butterfly chaotic attractors appear in the $x - w$ and $y - w$ phase planes. This coexistence can be better observed in Figures 1(g)–1(h). It can be concluded that system (1) can generate chaotic butterfly attractors of two-wing and four-wing at the same time.

## 3. Some Basic Properties of New System

*3.1. Symmetric and Dissipative Properties.* The Sprott B system is symmetric about the $z$-axis, and system (1) is also symmetric about the $z$-axis. A simple proof is shown in the following equation:

$$\begin{cases} \dot{x} = a(y - x) \\ \dot{y} = xz + w \\ \dot{z} = b - xy \\ \dot{w} = yz - cw \end{cases} \Longleftrightarrow \begin{cases} -\dot{x} = a(-y - (-x)) = -a(y - x), \\ -\dot{y} = (-x)z + (-w) = -xz - w, \\ \dot{z} = b - (-x)(-y) = b - xy, \\ -\dot{w} = (-y)z - c(-w) = -yz + cw. \end{cases} \tag{3}$$

The state space of system (1) is four-dimensional, so the vector field of system (1) is defined as follows:

$$f[X] = \begin{bmatrix} f_1(X) \\ f_2(X) \\ f_3(X) \\ f_4(X) \end{bmatrix} = \begin{bmatrix} ay - ax \\ xz + w \\ b - xy \\ yz - cw \end{bmatrix}. \tag{4}$$

The divergence of system (1) is obtained from the vector field as follows:

$$\nabla V = \frac{\partial f_1}{\partial x} + \frac{\partial f_2}{\partial y} + \frac{\partial f_3}{\partial z} + \frac{\partial f_4}{\partial w} = -(a + c). \tag{5}$$

According to equation (5), as long as $(a + c) > 0$, system (1) is dissipative, and the system converges in exponential form $\mathrm{d}V/\mathrm{d}t = e^{-(a+c)t}$. As $t \longrightarrow \infty$, all trajectories of the system will eventually be restricted to a set with a volume of zero, and the extreme motion will converge to an attractor, thus proving the existence of the attractors of the system.

*3.2. Equilibria and Stability.* In order to obtain the equilibrium points of system (1), let the right side of the equation be equal to zero. The system of equations is as follows:

$$\begin{cases} a(y - x) = 0, \\ xz + w = 0, \\ b - xy = 0, \\ yz - cw = 0. \end{cases} \tag{6}$$

By calculation, we get that the two equilibrium points of system (1) are $S_1 = (\sqrt{b}, \sqrt{b}, 0, 0)$ and $S_2 = (-\sqrt{b}, -\sqrt{b}, 0, 0)$. System (1) has the same characteristic equation at $S_{1,2}$:

$$\lambda^4 + (a + c)\lambda^3 + (b + ac)\lambda^2 + (2ab + bc + b)\lambda + 2abc + 2ab = 0. \tag{7}$$

According to the classical Routh–Hurwitz stability criterion, if $a > 0$, $b > 0$, and $c > 0$, the equilibrium points $S_{1,2}$ is unstable.

Let $a = 6$, $b = 11$, and $c = 5$, we can get the equilibrium points $S_1 = (\sqrt{11}, \sqrt{11}, 0, 0)$ and $S_2 = (-\sqrt{11}, -\sqrt{11}, 0, 0)$. For the first equilibrium point $S_1 = (\sqrt{11}, \sqrt{11}, 0, 0)$, system (1) is linearized to Jacobian matrix as follows:

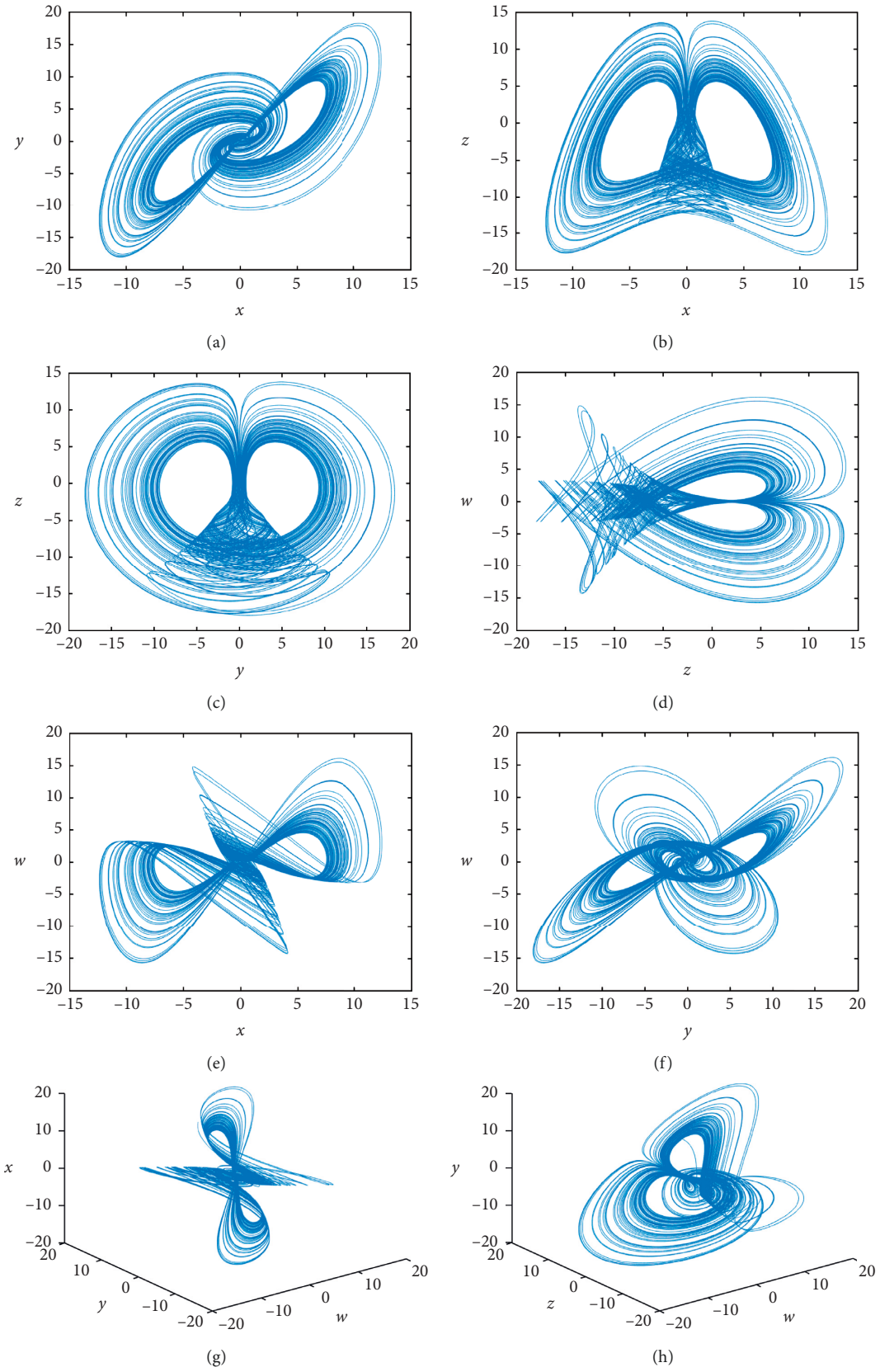


Figure 1: The two-wing butterfly chaotic attractors of system (1): (a) $x - y$, (b) $x - z$, (c) $y - z$, and (d) $z - w$. The four-wing butterfly chaotic attractors of system (1): (e) $x - w$ and (f) $y - w$. The coexisting chaotic attractors of system (1): (g) $x - y - w$ and (h) $y - z - w$.

$$J_1 = \begin{bmatrix} -a & a & 0 & 0 \\ z & 0 & x & 1 \\ -y & -x & 0 & 0 \\ 0 & z & y & -c \end{bmatrix} = \begin{bmatrix} -6 & 6 & 0 & 0 \\ 0 & 0 & \sqrt{11} & 1 \\ -\sqrt{11} & -\sqrt{11} & 0 & 0 \\ 0 & 0 & \sqrt{11} & -5 \end{bmatrix}. \quad (8)$$

Let $|\lambda I - J_1| = 0$, the eigenvalues of Jacobian matrix are as follows:

$$\begin{aligned} \lambda_1 &= 0.7301 + 4.4609i, \\ \lambda_2 &= 0.7301 - 4.4609i, \\ \lambda_3 &= -6, \\ \lambda_4 &= -6.4602. \end{aligned} \quad (9)$$

It can be seen that $\lambda_3$ and $\lambda_4$ are negative real numbers, $\lambda_1$ and $\lambda_2$ are a pair of conjugate complex numbers, and the real part is positive, so the equilibrium point $S_1$ is a saddle-focus, and system (1) is unstable at $S_1$.

For the second equilibrium point $S_2 = (-\sqrt{11}, -\sqrt{11}, 0, 0)$, system (1) is linearized to Jacobian matrix as follows:

$$J_2 = \begin{bmatrix} -a & a & 0 & 0 \\ z & 0 & x & 1 \\ -y & -x & 0 & 0 \\ 0 & z & y & -c \end{bmatrix} = \begin{bmatrix} -6 & 6 & 0 & 0 \\ 0 & 0 & -\sqrt{11} & 1 \\ \sqrt{11} & \sqrt{11} & 0 & 0 \\ 0 & 0 & -\sqrt{11} & -5 \end{bmatrix}. \quad (10)$$

In the same way, let $|\lambda I - J_2| = 0$, the eigenvalue obtained is shown in equation (9), so the equilibrium point $S_2$ is also a saddle-focus, and system (1) is unstable at $S_2$. Obviously, two saddle-foci are the key to the chaotic motion of system (1).

*3.3. Bifurcation Diagrams, Lyapunov Exponents, and Period-Doubling Bifurcation Process.* The dynamic behaviors of system (1) can be further analyzed by bifurcation diagrams, Lyapunov exponents, and period-doubling bifurcation process.

Let $a = 6$, $c = 5$, and $b \in [9, 20]$. We draw the bifurcation diagrams of the $z$ peak of system (1) changing with $b$, as shown in Figure 2(a). In Figure 2(a), the red and blue branches represent the different attractors generated from different initial values $X^+ = (10, 10, 0, 0)$ and $X^- = (-10, -10, 0, 0)$, and the overlapped parts represent the same attractors generated. As $b$ increases in $[12, 20]$, the bifurcation diagrams clearly show the trajectory of system (1) from classical period-doubling bifurcation to chaos. Figures 2(b) and 2(c) show the Lyapunov exponents of system (1) which changes with the increase of parameter $b$, where $LE_1 > LE_2 > LE_3 > LE_4$. By comparing the three diagrams, it can be seen that the bifurcation diagrams are completely consistent with the dynamic behaviors described by Lyapunov exponents.

Figures 3(a)–3(d) describe in detail the main orbital states through which system (1) operates. When $b = 13.6$, system (1) has a pair of period-1 attractors. When $b = 14.5$, system (1) has a pair of period-2 attractors. When $b = 15$, system (1) has a pair of strange attractors. When $b = 18.5$, system (1) has a strange attractor.

Table 1 shows the comparison of the Lyapunov exponents of the new system with the literature [12, 28–30]. It can be seen that the maximum $LE_1$ of the new system is larger. It indicates that the chaotic characteristics of the new system are more obvious, the chaotic degree is higher, and the dynamic characteristics of the system are more difficult to predict.

*3.4. Coexisting Attractors.* Let $a = 10$, $b = 10$, and $c \in [0, 6]$, and we draw the bifurcation diagrams of the $x$ peak of system (1) changing with parameter $c$. Similarly, the red and blue branches in Figure 4(a), respectively, represents the different attractors generated from different initial values of $X^+ = (10, 10, 0, 0)$ and $X^- = (-10, -10, 0, 0)$, and the overlaps represent the same attractors generated. Figures 4(b) and 4(c) show the Lyapunov exponents of system (1) changing with the increase of parameter $c$. It is obvious that $LE_1 > LE_2 > LE_3 > LE_4$. Figure 4 shows that periodic attractors, chaotic attractors, and coexisting attractors exist in system (1).

Figure 4(a) not only shows that system (1) has coexisting attractors but also shows that with the increase of $c$ in $[1, 4.18]$, system (1) shows a trajectory from reverse period-doubling bifurcation to chaos. Figures 5(a)–5(d) describe the major orbital states of ergodic when symmetrically coexisting attractors appear in system (1). When $c = 1.55$, the system gets a pair of strange attractors. When $c = 1.92$, the system has a pair of period-2 attractors. When $c = 2.01$, the system has a pair of period-1 attractors. When $c = 4.3$, the system also has a pair of strange attractors. Figures 4(b)–4(c) Lyapunov exponents verify the above process and determine the property of the attractors.

Figure 6 is a dynamical map, mainly depicting the influence of changing parameters $b$ and $c$ on the dynamical map characteristics of the system. Taking the relationship between the maximum Lyapunov exponent and 0 as the standard, the blue region represents the chaotic state of the system, and the maximum Lyapunov exponent is greater than 0; the yellow region represents the periodic state, and the maximum Lyapunov exponent is equal to 0; and the red region represents the system is stable under this parameter condition, and the maximum Lyapunov exponent is less than 0. It can be seen from the figure that as the parameter $c$ increases, the system state alternates between chaotic state and periodic state and occasionally tends to be stable.

## 4. Circuit Implementation

In order to verify the dynamic behaviors of chaotic system, an actual circuit is designed to realize the chaotic system according to equation (1). The circuit is mainly realized by linear resistances of different resistance values, linear capacitances, operational amplifier TL082IP, and multiplier AD633. However, it should be noted that in the actual circuit, the allowable voltage range of the analog multiplier is

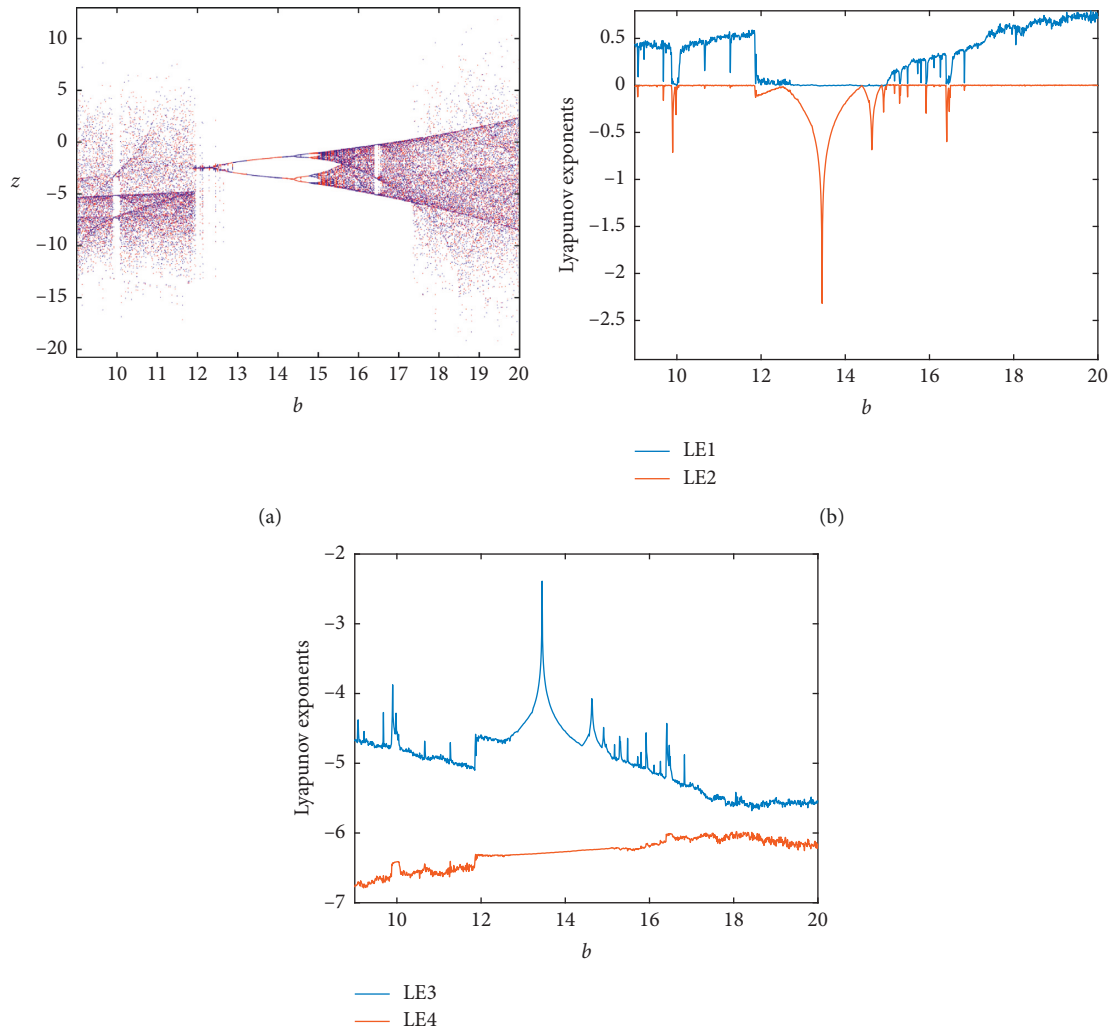


Figure 2: Bifurcation diagrams and Lyapunov exponential spectrums of system (1) when $a = 6$, $c = 5$, and $b \in [9, 20]$: (a) bifurcation diagrams of $z$ peak changing with parameter $b$; (b) $LE_1$ and $LE_2$; (c) $LE_3$ and $LE_4$.

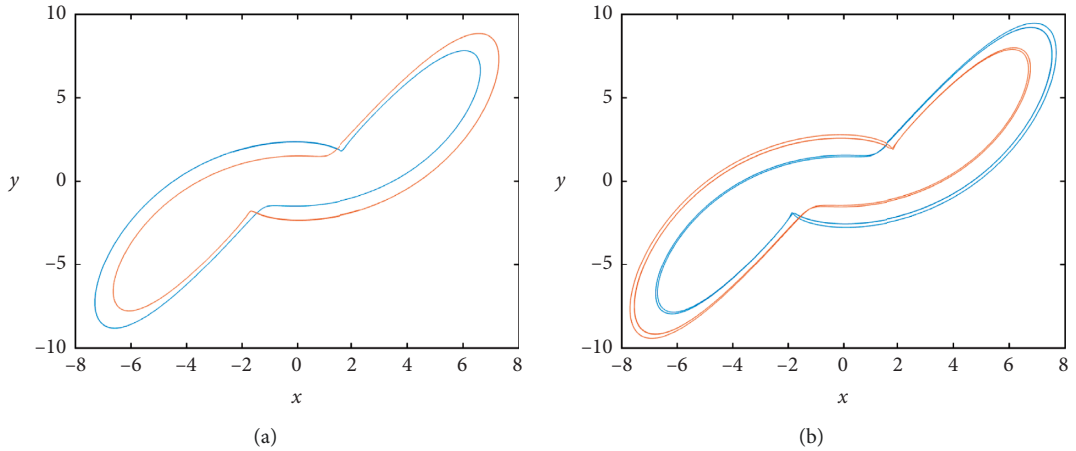


Figure 3: Continued.

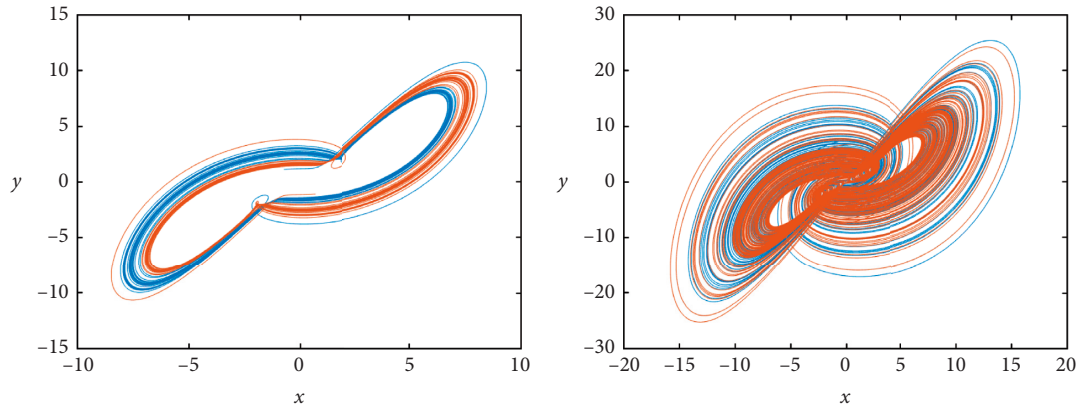


Figure 3: Attractors of system (1) with $a = 6$ and $c = 5$: (a) $b = 13.6$, (b) $b = 14.5$, (c) $b = 15$, and (d) $b = 18.5$.

Table 1: The Lyapunov exponents of five systems.

| Name | System | Parameter values | Lyapunov exponents |
|---|---|---|---|
| Sprott B system | $\dot{x} = yz$<br>$\dot{y} = x - y$<br>$\dot{z} = 1 - xy$ | None | $LE_1 = 0.210$<br>$LE_2 = 0$<br>$LE_3 = -1.210$ |
| Li system | $\dot{x} = y - x$<br>$\dot{y} = -xz + u$<br>$\dot{z} = xy - a$<br>$\dot{u} = -by$ | $a = 2.6$<br>$b = 0.44$ | $LE_1 = 0.070$<br>$LE_2 = 0.013$<br>$LE_3 = 0$<br>$LE_4 = -1.083$ |
| Lai system | $\dot{x} = a(y - x)$<br>$\dot{y} = xz - xw$<br>$\dot{z} = b - xy$<br>$\dot{w} = c\mathrm{sgn}(z) - kw$ | $a = 1$<br>$b = 1$<br>$c = 9$<br>$k = 2$ | $LE_1 = 0.211$<br>$LE_2 = 0$<br>$LE_3 = -1.210$<br>$LE_4 = -2$ |
| Zhou system | $\dot{x} = a(w - x)$<br>$\dot{y} = -by + zw$<br>$\dot{z} = cx - xw$<br>$\dot{w} = dy - z + xz$ | $a = 2$<br>$b = 3.9$<br>$c = 3$<br>$d = 1$ | $LE_1 = 0.092$<br>$LE_2 = 0$<br>$LE_3 = -1.988$<br>$LE_4 = -4.004$ |
| New system | $\dot{x} = a(y - x)$<br>$\dot{y} = xz + w$<br>$\dot{z} = b - xy$<br>$\dot{w} = yz - cw$ | $a = 6$<br>$b = 11$<br>$c = 5$ | $LE_1 = 0.516$<br>$LE_2 = 0$<br>$LE_3 = -4.921$<br>$LE_4 = -6.595$ |

$\pm 10$ V and the allowable voltage range of the operational amplifier is $\pm 18$ V. The dynamic range of variables $x$, $y$, $z$, and $w$ are approximately $[-15, 15]$, $[-20, 20]$, $[-20, 15]$, and $[-20, 20]$, respectively. It is beyond the allowable voltage range of analog multipliers and operational amplifiers, so it is necessary to make appropriate variable proportional compression transformation to the system state variables, so as to facilitate the implementation of the circuit. System (1) is transformed by proportional compression of uniform variables, so that $x$, $y$, $z$, and $w$ are compressed to the original 1/5, which is $(x, y, z, w) \longrightarrow (5x, 5y, 5z, 5w)$. The chaotic system equation after transformation is as follows:

$$\begin{cases} \dfrac{dx}{dt} = a(y - x) \\ \dfrac{dy}{dt} = xz + w \\ \dfrac{dz}{dt} = b - xy \\ \dfrac{dw}{dt} = yz - cw \end{cases} = \begin{cases} \dfrac{d(5x)}{dt} = a(5y - 5x) \\ \dfrac{d(5y)}{dt} = 5x \cdot 5z + 5w \\ \dfrac{d(5z)}{dt} = b - 5x \cdot 5y \\ \dfrac{d(5w)}{dt} = 5y \cdot 5z - 5cw \end{cases} = \begin{cases} \dfrac{dx}{dt} = ay - ax, \\ \dfrac{dy}{dt} = 5xz + w, \\ \dfrac{dz}{dt} = \dfrac{b}{5} - 5xy, \\ \dfrac{dw}{dt} = 5yz - cw. \end{cases} \tag{11}$$

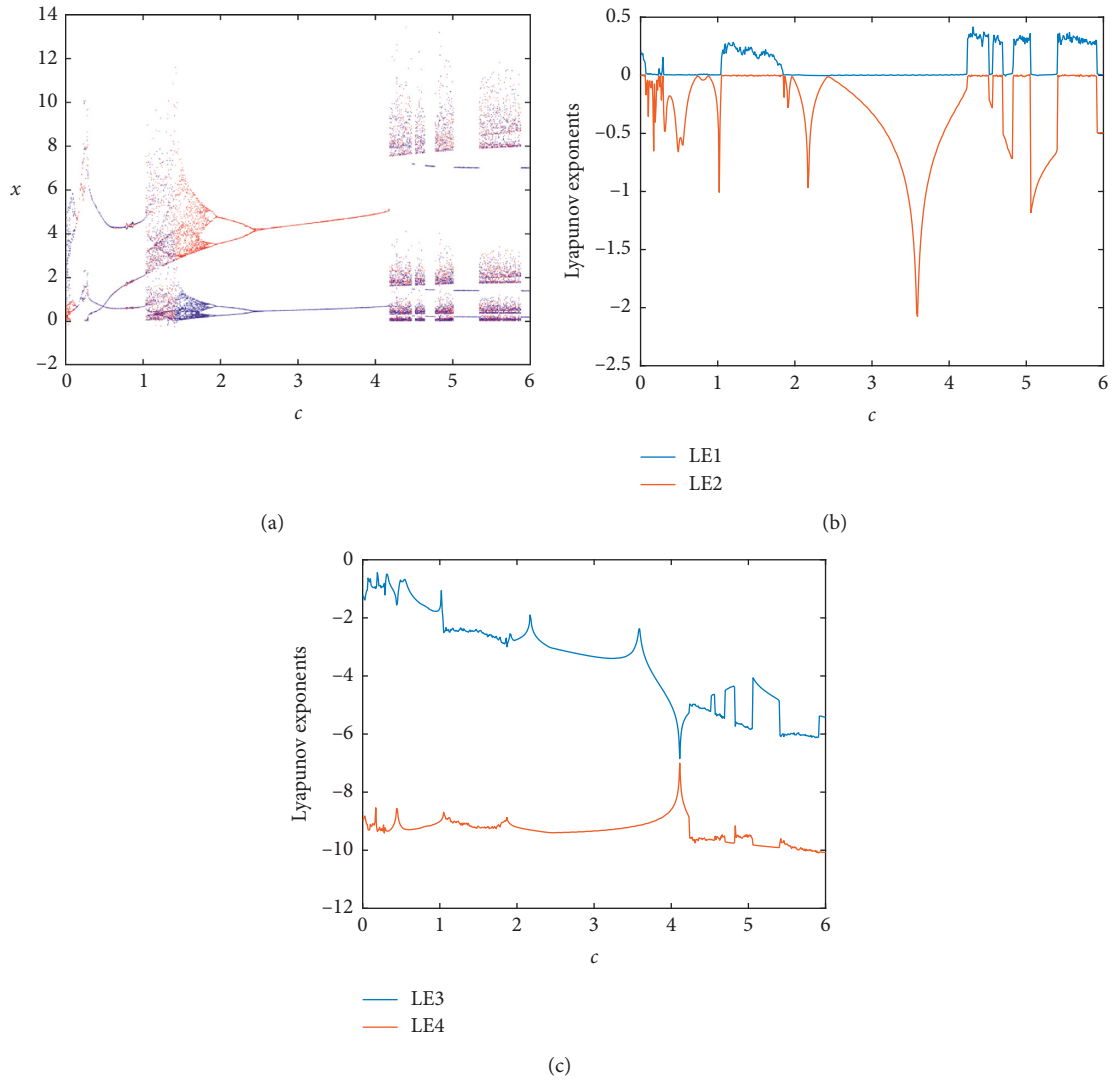


Figure 4: Bifurcation diagrams and Lyapunov exponential spectrums of system (1) when $a = 10$, $b = 10$, and $c \in [0, 6]$: (a) bifurcation diagrams of $x$ peak changing with parameter $c$; (b) $LE_1$ and $LE_2$; (c) $LE_3$ and $LE_4$.

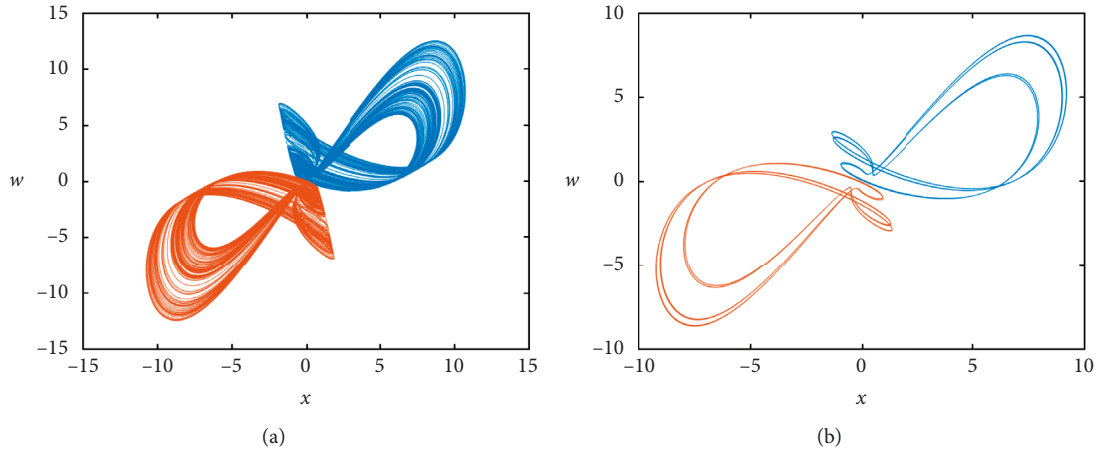


Figure 5: Continued.

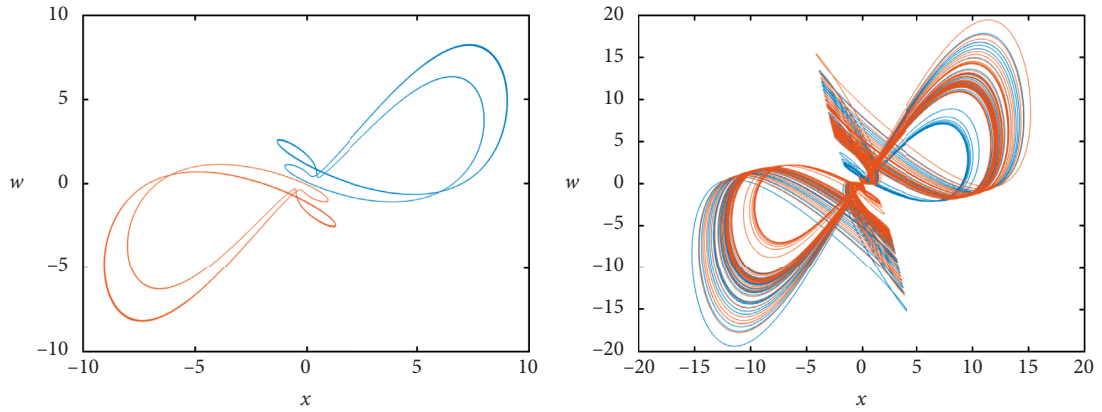


Figure 5: Attractors of system (1) with $a = 10$ and $b = 10$: (a) $c = 1.55$, (b) $c = 1.92$, (c) $c = 2.01$, and (d) $c = 4.3$.

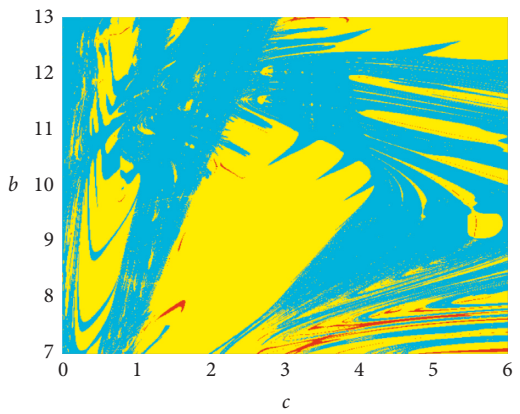


Figure 6: Dynamical map with respect to parameters $b$ and $c$.

In this way, the amplitude of the output chaotic signal can be reduced to 1/5 of the original system.

Make time-scale transformation of equation (11), and transform $t$ into $\tau_0 t$ in the equation, where $\tau_0 = 100$, and the results are as follows:

$$\begin{cases} \dfrac{dx}{dt} = 100ay - 100ax, \\ \dfrac{dy}{dt} = 500xz + 100w, \\ \dfrac{dz}{dt} = 20b - 500xy, \\ \dfrac{dw}{dt} = 500yz - 100cw. \end{cases} \tag{12}$$

The modular circuit is designed according to the above formula, as shown in Figure 7.

According to the circuit schematic diagrams, the corresponding self-excited oscillation circuit equation is obtained as follows:

$$\begin{cases} \dfrac{dx}{dt} = -\dfrac{R_3}{R_2R_4C_1}(-y) - \dfrac{R_3}{R_1R_4C_1}x, \\ \dfrac{dy}{dt} = -\dfrac{R_9}{R_7R_{10}C_2}(-w) - \dfrac{R_9}{10R_8R_{10}C_2}(-x)z, \\ \dfrac{dz}{dt} = -\dfrac{R_{15}}{R_{13}R_{16}C_3}(-1) - \dfrac{R_{15}}{10R_{14}R_{16}C_3}xy, \\ \dfrac{dw}{dt} = -\dfrac{R_{21}}{R_{19}R_{22}C_4}w - \dfrac{R_{21}}{10R_{20}R_{22}C_4}y(-z). \end{cases} \tag{13}$$

By comparing equation (12) with equation (13), we can get

$$\begin{aligned} a &= \frac{R_3}{100R_1R_4C_1} = \frac{R_3}{100R_2R_4C_1}, \\ 500 &= \frac{R_9}{10R_8R_{10}C_2}, \\ 100 &= \frac{R_9}{R_7R_{10}C_2}, \\ b &= \frac{R_{15}}{20R_{13}R_{16}C_3}, \\ 500 &= \frac{R_{15}}{10R_{14}R_{16}C_3}, \\ 500 &= \frac{R_{21}}{10R_{20}R_{22}C_4}. \\ c &= \frac{R_{21}}{100R_{19}R_{22}C_4}, \end{aligned} \tag{14}$$

In this paper, Multisim software is used for circuit simulation, in which the output scaling factor of the analog multiplier AD633 is set as 100 mV/1 V and the power supply voltage is ±12 V. The integral time constant of the four

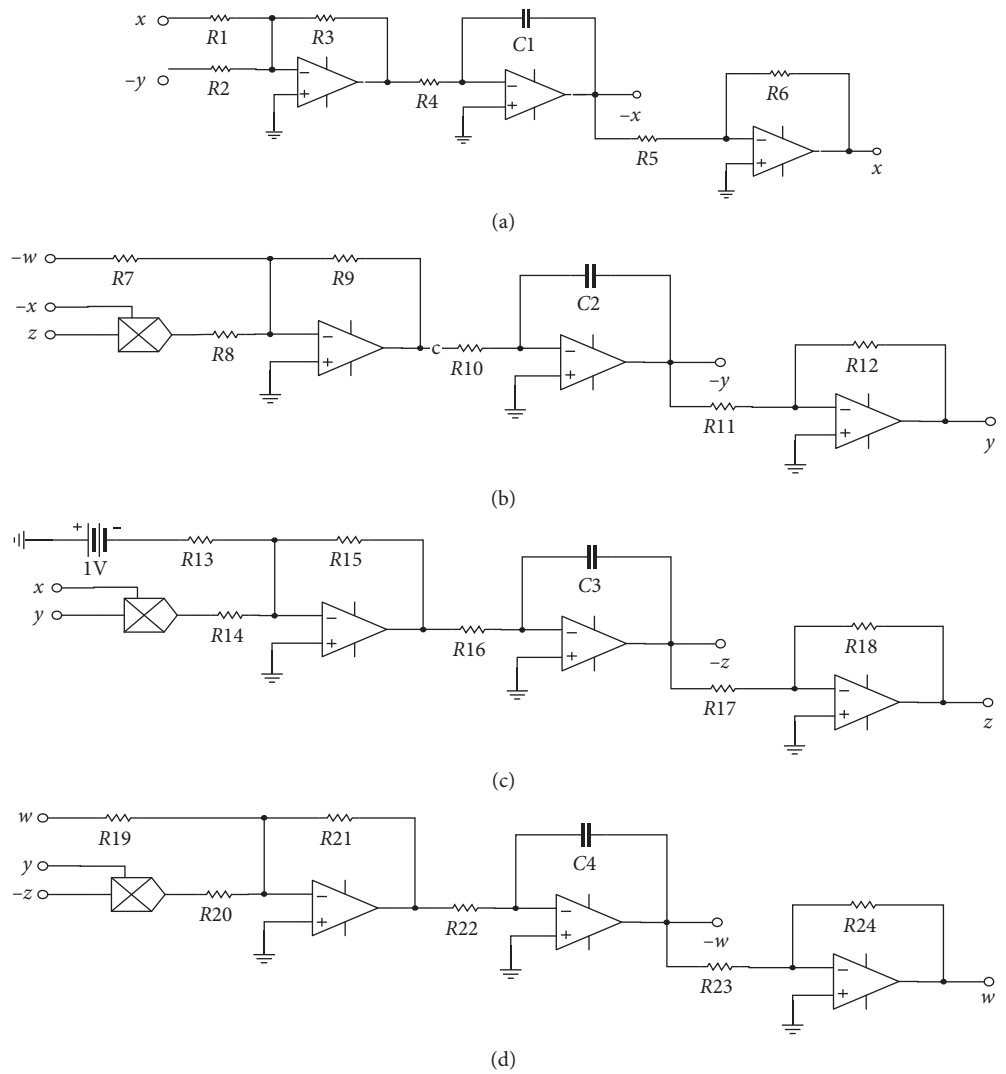


Figure 7: Schematic diagrams of chaotic circuit: (a) variable $x$ equivalent circuit, (b) variable $y$ equivalent circuit, (c) variable $z$ equivalent circuit, and (d) variable $w$ equivalent circuit.

circuit channels can be changed by adjusting the capacitance; set $C_1 = C_2 = C_3 = C_4 = 10\,\text{nF}$, $R_4 = R_{10} = R_{16} = R_{22} = 50\,k\Omega$, and $R_3 = R_5 = R_6 = R_9 = R_{12} = R_{15} = R_{17} = R_{18} = R_{21} = R_{23} = R_{24} = 100\,k\Omega$. When $a = 6$, $b = 11$, and $c = 5$, it can be obtained from equation (14) that $R_1 = R_2 = 333\,k\Omega$, $R_7 = 2000\,k\Omega$, $R_8 = R_{14} = R_{20} = 40\,k\Omega$, $R_{13} = 909\,k\Omega$, and $R_{19} = 400\,k\Omega$. Circuit simulation results are shown in Figure 8. These trajectories are consistent with numerical simulation results.

Similarly, we can use circuit simulations to observe the orbital states of system (1) as it moves towards chaos. Keep other parameters unchanged, and control the value of parameter $b$ by changing $R_{13}$. Figures 9(a)–9(d) describe the trajectories starting from the initial value $X^+(10, 10, 0, 0)$, where $R_{13} = 735\,k\Omega$ corresponds to parameter $b = 13.6$, $R_{13} = 690\,k\Omega$ corresponds to parameter $b = 14.5$, $R_{13} = 667\,k\Omega$ corresponds to parameter $b = 15$, and $R_{13} = 540\,k\Omega$ corresponds to $b = 18.5$. By comparing with Figure 3, it can be seen that the results of circuit simulation and numerical simulation are consistent.

The following circuit simulation is used to verify the symmetric coexisting attractors in system (1), mainly verifying the first three orbital states. Because the parameters have changed, the value of the corresponding resistances in the circuit should also be changed. Equation (14) can be used to calculate the corresponding resistances $R_1 = R_2 = 200\,k\Omega$ and $R_{13} = 1000\,k\Omega$ when $a = 10$ and $b = 10$. The parameter $c$ is controlled by the resistance $R_{19}$. $c = 1.55 \longrightarrow R_{19} = 1290\,k\Omega$, $c = 1.92 \longrightarrow R_{19} = 1042\,k\Omega$, and $c = 2.01 \longrightarrow R_{19} = 995\,k\Omega$. The left graph of Figure 10 shows the attractors starting from initial value $X^+(10, 10, 0, 0)$, and the right graph of Figure 10 shows the attractors starting from initial value $X^-(-10, -10, 0, 0)$. By comparing the circuit simulation diagrams with the numerical simulation diagrams in the previous section, we can see that the experimental results of the two are in good agreement.

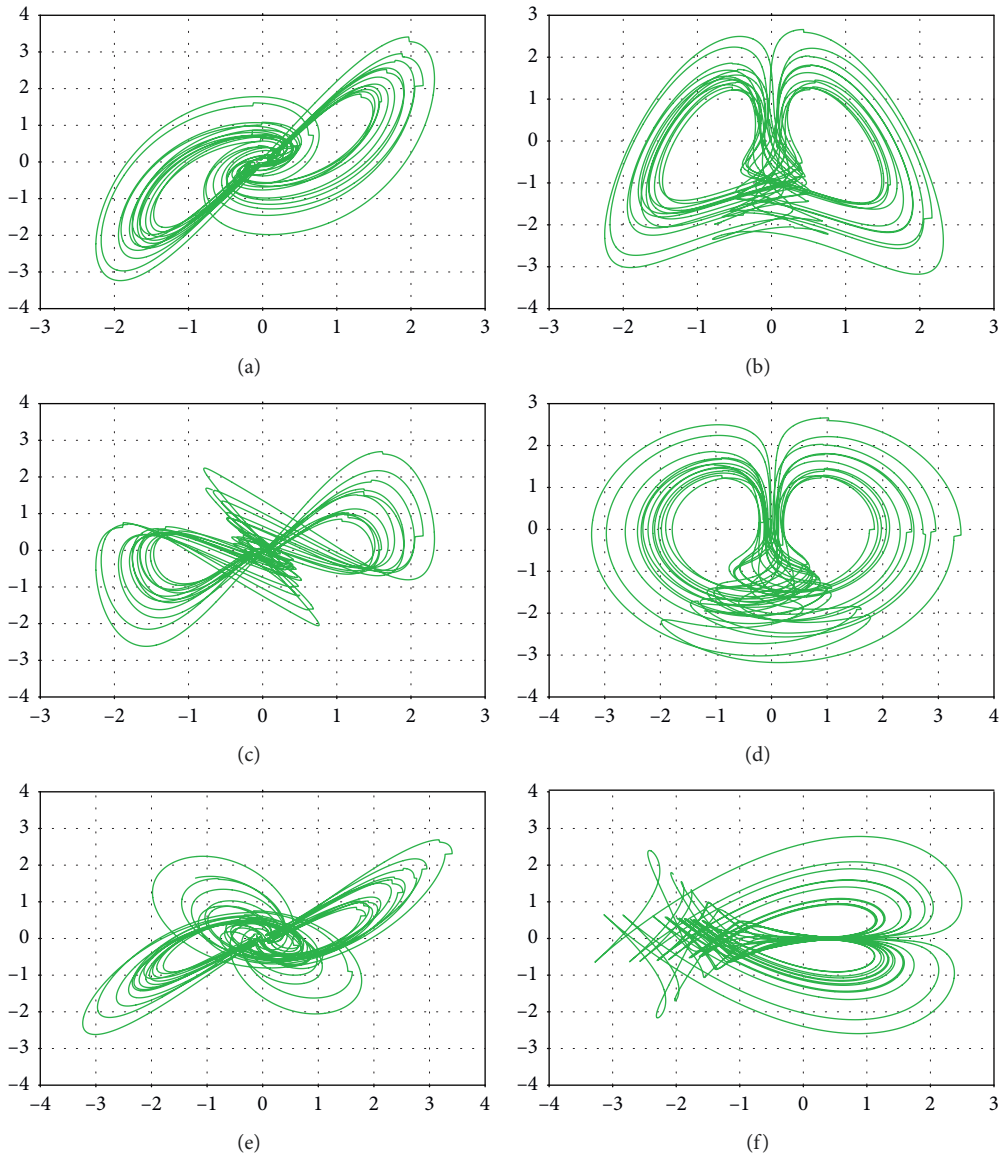


Figure 8: The circuit realization of phase diagrams for system (1): (a) $x - y$, (b) $x - z$, (c) $x - w$, (d) $y - z$, (e) $y - w$, and (f) $z - w$.

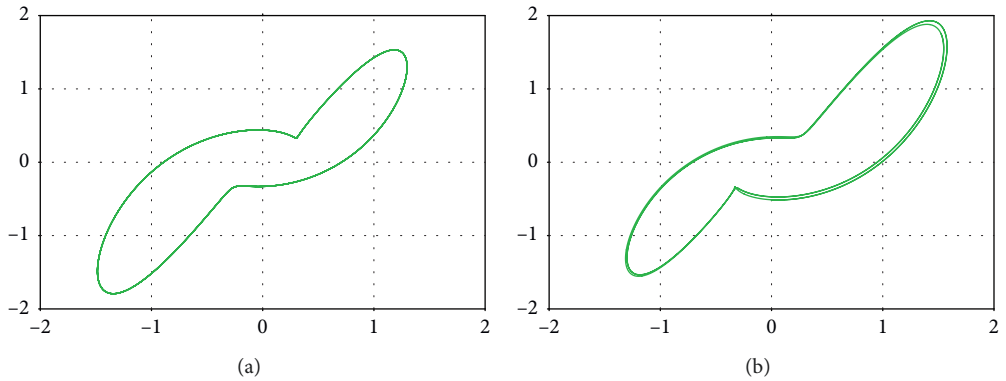


Figure 9: Continued.

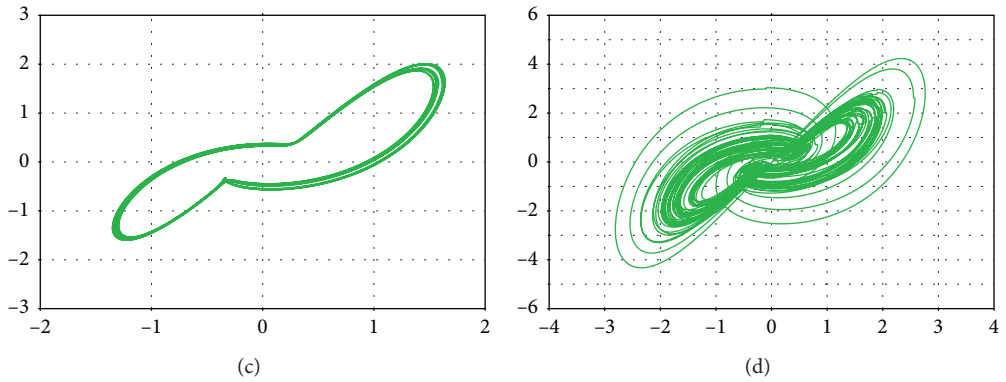


FIGURE 9: The circuit realization of attractors for system (1): (a) $R_{13} = 735\,k\Omega$, (b) $R_{13} = 690\,k\Omega$, (c) $R_{13} = 667\,k\Omega$, and (d) $R_{13} = 540\,k\Omega$.

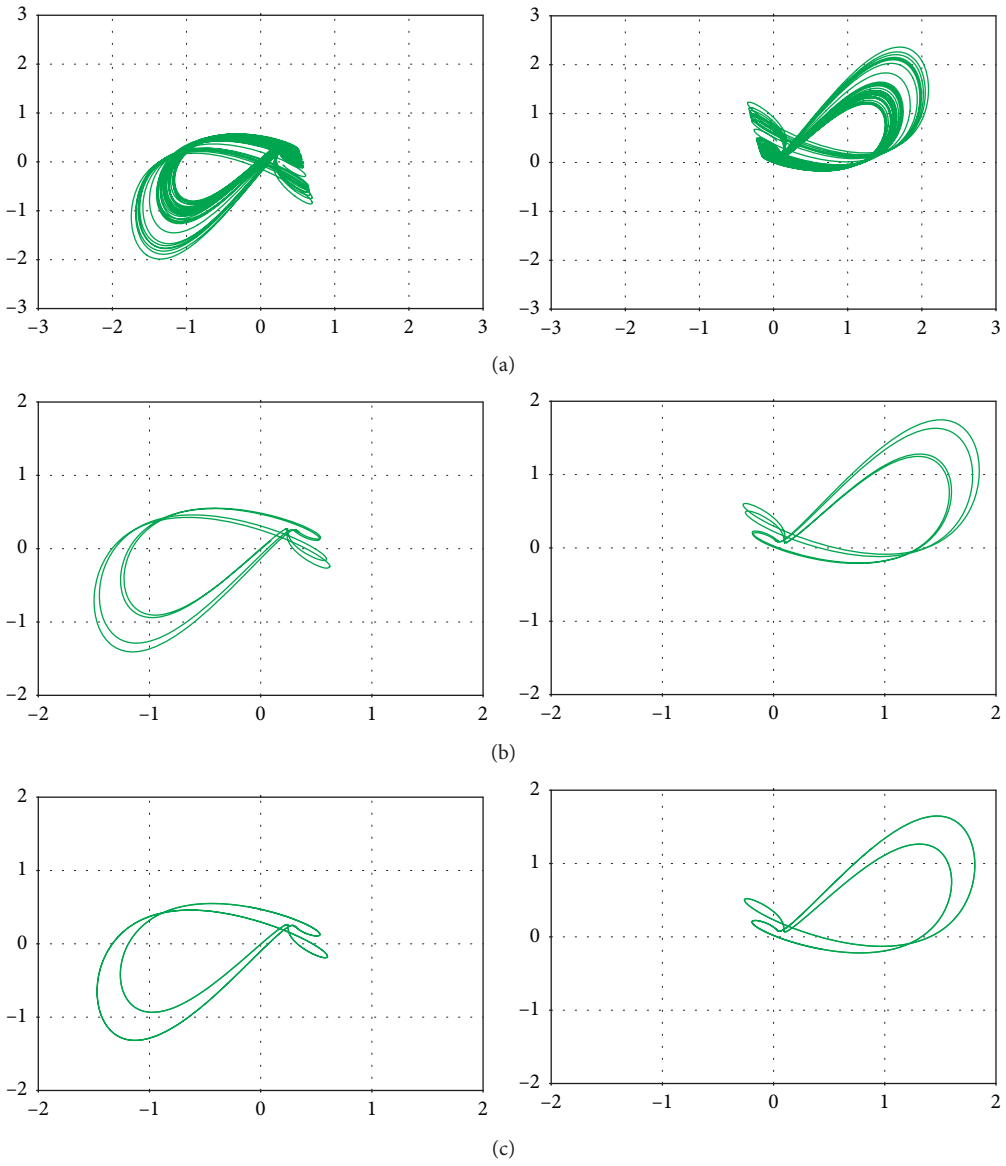


FIGURE 10: The attractors of system (1) from initial value $X^+(10, 10, 0, 0)$ (left) and attractors from initial value $X^-(-10, -10, 0, 0)$ (right): (a) $R_{19} = 1290\,k\Omega$, (b) $R_{19} = 1042\,k\Omega$, and (c) $R_{19} = 995\,k\Omega$.

## 5. Conclusion

In this paper, a new four-dimensional chaotic system is designed by adding a state-feedback controller to the Sprott B system. It contains three nonlinear terms and one constant term and is symmetric about $z$-axis. Through the analysis of system diagrams, bifurcation diagrams, and Lyapunov exponents, it is found that the new system can generate not only two-wing and four-wing attractors but also symmetrical coexisting attractors, and the complexity of the system is further improved. We also design the electronic circuit, and the results of the circuit simulation experiment are consistent with those of the numerical simulation experiment, which proves the correctness of the theoretical analysis and the realizability of the system. The dynamic characteristics of the new system are more abundant, and it has great prospects in the fields of image encryption and secure communication.

## Data Availability

The data used to support the findings of this study are included within the article.

## Conflicts of Interest

The authors declare no conflicts of interest.

## Acknowledgments

This research was funded by the National Natural Science Foundation of China (Nos. 61203004 and 61306142) and Natural Science Foundation of Heilongjiang Province (Grant no. F201220).

## References

[1] J. Gleick and R. C. Hilborn, "Chaos, making a new science," *American Journal of Physics*, vol. 56, no. 11, p. 79, 1998.

[2] M. Hasler, "Chaotic behaviour in electronic circuits || engineering chaos for encryption and broadband communication," *Philosophical Transactions: Physical Sciences and Engineering*, vol. 353, no. 1701, pp. 115–126, 1995.

[3] A. V. Oppenheim, G. W. Wornell, S. H. Isabelle, and K. M. Cuomo, "Signal processing in the context of chaotic signals," in *Proceedings of the IEEE International Conference on Acoustics, Speech, and Signal Processing*, pp. 117–120, San Francisco, CA, USA, March 1992.

[4] T. Elbert, W. J. Ray, Z. J. Skinner, J. E. Skinner, K. E. Graf, and N. Birbaumer, "Chaos and physiology: deterministic chaos in excitable cell assemblies," *Physiological Reviews*, vol. 74, no. 1, pp. 1–47, 1994.

[5] L. J. Yang and T. L. Chen, "Application of chaos in genetic algorithms," *Communications in Theoretical Physics*, vol. 38, no. 2, pp. 168–172, 2002.

[6] V. P. Maslov, "Theory of chaos and its application to the crisis of debts and the origin of inflation," *Russian Journal of Mathematical Physics*, vol. 16, no. 1, pp. 103–120, 2009.

[7] G. CHEN and L. Ü Jinhu, *Dynamics Analysis, Control and Synchronization of Lorenz System Family*, Science Press, Beijing, China, 2003.

[8] E. N. Lorenz, "Deterministic nonperiodic flow," *Journal of the Atmospheric Sciences*, vol. 20, no. 2, pp. 130–141, 1963.

[9] O. E. Rössler, "An equation for continuous chaos," *Physics Letters A*, vol. 57, no. 5, pp. 397-398, 1976.

[10] L. Chua, M. Komuro, and T. Matsumoto, "The double scroll family," *IEEE Transactions on Circuits and Systems*, vol. 33, no. 11, pp. 1072–1118, 1986.

[11] R. N. Madan, *Chua's Circuit: A Paradigm for Chaos*, World Scientific, Singapore, 1993.

[12] J. C. Sprott, "Some simple chaotic flows," *Physical Review E*, vol. 50, no. 2, pp. 647–650, 1994.

[13] G. Chen and T. Ueta, "Yet another chaotic attractor," *International Journal of Bifurcation and Chaos*, vol. 9, no. 7, pp. 1465-1466, 1999.

[14] J. Lü, G. Chen, S. Zhang et al., "Dynamical analysis of a new chaotic attractor," *International Journal of Bifurcation and Chaos*, vol. 12, no. 05, pp. 1001–1015, 2002.

[15] W. Liu and G. Chen, "A new chaotic system and its generation," *International Journal of Bifurcation and Chaos*, vol. 13, no. 1, pp. 261–267, 2003.

[16] J. Kengne, Z. T. Njitacke, H. B. Fotsin et al., "Dynamical analysis of a simple autonomous jerk system with multiple attractors," *Nonlinear Dynamics*, vol. 83, no. 1-2, pp. 751–765, 2016.

[17] X. Wang, S. Vaidyanathan, C. Volos, V.-T. Pham, and T. Kapitaniak, "Dynamics, circuit realization, control and synchronization of a hyperchaotic hyperjerk system with coexisting attractors," *Nonlinear Dynamics*, vol. 89, no. 3, pp. 1673–1687, 2017.

[18] X. Wang, X. Min, J. Yu, Y. Shen, G. Wang, and H. C. I. Ho, "Realization of a novel logarithmic chaotic system and its characteristic analysis," *International Journal of Bifurcation and Chaos*, vol. 29, no. 2, Article ID 1930004, 2019.

[19] L. Wang, "3-scroll and 4-scroll chaotic attractors generated from a new 3-D quadratic autonomous system," *Nonlinear Dynamics*, vol. 56, no. 4, pp. 453–462, 2009.

[20] B. Bao, J. Xu, Z. Liu, and Z. Ma, "Hyperchaos from an augmented Lü system," *International Journal of Bifurcation and Chaos*, vol. 20, no. 11, pp. 3689–3698, 2010.

[21] P. Li, J. Xu, J. Mou et al., "Fractional-order 4D hyperchaotic memristive system and application in color image encryption," *EURASIP Journal on Image and Video Processing*, vol. 2019, no. 1, pp. 1–11, 2019.

[22] N. Okafor, B. Zahawi, D. Giaouris, and S. Banerjee, "Chaos, coexisting attractors, and fractal basin boundaries in DC drives with full-bridge converter," in *Proceedings of the 2010 IEEE International Symposium on Circuits and Systems*, pp. 129–132, Paris, France, May-June 2010.

[23] G. A. Leonov, N. V. Kuznetsov, and V. I. Vagaitsev, "Hidden attractor in smooth Chua systems," *Physica D: Nonlinear Phenomena*, vol. 241, no. 18, pp. 1482–1486, 2012.

[24] J. C. Sprott, X. Wang, and G. Chen, "Coexistence of point, periodic and strange attractors," *International Journal of Bifurcation and Chaos*, vol. 23, no. 5, Article ID 1350093, 2013.

[25] Z. P. Peng, C. H. Wang, Y. Lin et al., "A novel four-dimensional multi-wing hyper-chaotic attractor and its application in image encryption," *Acta Physica Sinica*, vol. 63, no. 24, pp. 97–106, 2014.

[26] F. Z. Wang, G. Y. Qi, Z. Q. Chen et al., "On a four-winged chaotic attractor," *Acta Physica Sinica*, vol. 56, no. 6, pp. 3137–3144, 2007.

[27] C. Li and J. C. Sprott, "Multistability in a butterfly flow," *International Journal of Bifurcation and Chaos*, vol. 23, no. 12, Article ID 1350199, 2013.

[28] C. Li and J. C. Sprott, "Coexisting hidden attractors in a 4-D simplified Lorenz system," *International Journal of Bifurcation and Chaos*, vol. 24, no. 03, Article ID 1450034, 2014.
[29] Q. Lai, A. Akgul, X.-W. Zhao, and H. Pei, "Various types of coexisting attractors in a new 4D autonomous chaotic system," *International Journal of Bifurcation and Chaos*, vol. 27, no. 9, Article ID 1750142, 2017.
[30] C. Zhou, C. Yang, D. Xu, and C. Chen, "Coexisting attractors, circuit realization and impulsive synchronization of a new four-dimensional chaotic system," *Modern Physics Letters B*, vol. 33, no. 3, Article ID 1950026, 2019.